INVESTIGATION OF A HORIZONTAL RECTANGULAR SLOT ON CONDUCTING SPHERE USING DYADIC GREEN FUNCTION APPROACH

Chuwong Phongcharoenpanich, Damrong Boonrod, Phairote Wounchoum, and Monai Krairiksh
Faculty of Engineering and Research Center for Communications and Information Technology,
King Mongkut's Institute of Technology Ladkrabang, Bangkok 10520 Thailand,
Phone: (662) 7373000 Ext.3346 Fax: (662) 7392429 E-mail: kpchuwon@kmitl.ac.th

1. Introduction

Wireless communication systems are growing rapidly. In these systems, an antenna plays an important role in establishing a communication link between different destination points. With diversified applications of wireless communications, the demands of complicated antennas have increased and they must fulfill a number of additional requirements. Such antenna must feature improved performance, including attracting the commercial market. This paper is to investigate the characteristics of a horizontal rectangular slot on a conducting sphere that is proposed for applying for point to point communication. The influenced parameter to the radiation is the radius of a conducting sphere. The dyadic Green function approach is used to analyze the electromagnetic fields radiating from the slot. The sinusoidal voltage distribution along the slot is reasonably assumed. The far-field expressions can be derived by using the asymptotic formulas of spherical Hankel functions and the continuous fields at the slot orientation. The numerical results of radiation characteristics such as radiation pattern, half-power beamwidth, directivity, front-to-back ratio are also demonstrated.

2. Geometry of the Problem

The geometry of the problem is composed of the rectangular slot of the length of *2l* and the width of *2α*. The slot is horizontally oriented along the circumference of the conducting sphere of the redius *a* as shown in Fig.1.

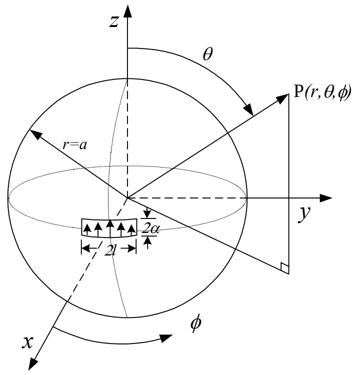

Fig.1 A horizontal rectangular slot on conducting sphere

3. Dyadic Green Function Approach

The dyadic Green function approach is a versatile tool for investigation of the region contained the source. This method is very popular lately due to the growth of high performance computer that can enhance the computation capability in calculation of the intricate formulas. In the calculation, the source has to be first considered. In the case of a horizontal rectangular slot on the conducting sphere, the equivalent magnetic current sheet along ϕ axis is considered as [1]

$$\bar{M}(\bar{R}') = -V\sin\left[\frac{2\pi}{\lambda}(l - a\phi')\right]\hat{\phi}, \quad \begin{cases} -l/a < \phi' < l/a \\ \theta_1 - \alpha < \theta' < \theta_1 + \alpha \end{cases} \tag{1}$$

The electric field due to the magnetic current source of (1) can be found using [2]

$$\bar{E}(r,\theta,\phi) = \iint \bar{\bar{G}}_{m1}(\bar{R},\bar{R}')\cdot[\bar{M}(\bar{R}')]ds' \tag{2}$$

The dyadic Green function plays significant parameters to realize the field due to the source. The dyadic Green functions after some intricate derivations can be as below.

ISBN: 89-86522-78-0 94460©KEES

$$\bar{\bar{G}}_{m1}(r,\theta,\phi;\, r',\theta',\phi') = -\frac{e^{-jkr}}{4\pi r}\sum_{n=0}^{\infty}\sum_{m=0}^{\infty} C_{mn} k(j^{n+1})\left\{ j\left(\bar{N}'(k) + a_n \bar{N}'^{(2)}(k)\right)\left(\mp\frac{m}{\sin\theta} P_n^m \cos(\theta) \begin{matrix}\sin\\ \cos\end{matrix} m\phi\hat{\theta} - \frac{\partial}{\partial\theta} P_n^m \cos(\theta) \begin{matrix}\cos\\ \sin\end{matrix} m\phi\hat{\phi}\right)\right.$$

$$\left. + \left(\bar{M}'(k) + b_n \bar{M}'^{(2)}(k)\right)\left(\frac{\partial}{\partial\theta} P_n^m \cos(\theta) \begin{matrix}\cos\\ \sin\end{matrix} m\phi\hat{\theta} \mp \frac{m}{\sin\theta} P_n^m \cos(\theta) \begin{matrix}\sin\\ \cos\end{matrix} m\phi\hat{\theta}\right)\right\} \tag{3}$$

where the vector wave functions are expressed as

$$\bar{M}'(k) = \left[\mp\frac{m}{\sin\theta'} j_n(kr') P_n^m \cos(\theta') \begin{matrix}\sin\\ \cos\end{matrix} m\phi'\hat{\theta} - j_n(kr')\frac{\partial}{\partial\theta'} P_n^m \cos(\theta') \begin{matrix}\cos\\ \sin\end{matrix} m\phi'\hat{\phi}\right] \tag{4}$$

$$\bar{M}'^{(2)}(k) = \left[\mp\frac{m}{\sin\theta'} h_n^{(2)}(kr') P_n^m \cos(\theta') \begin{matrix}\sin\\ \cos\end{matrix} m\phi'\hat{\theta} - h_n^{(2)}(kr')\frac{\partial}{\partial\theta'} P_n^m \cos(\theta') \begin{matrix}\cos\\ \sin\end{matrix} m\phi'\hat{\phi}\right] \tag{5}$$

$$\bar{N}'(k) = \left[\frac{n(n+1)}{kr'} j_n(kr') P_n^m \cos(\theta') \begin{matrix}\cos\\ \sin\end{matrix} m\phi'\hat{r} + \frac{1}{kr'}\frac{\partial}{\partial(kr')}\left[kr' j_n(kr')\right]\left(\frac{\partial}{\partial\theta'} P_n^m \cos(\theta') \begin{matrix}\cos\\ \sin\end{matrix} m\phi'\hat{\theta} \mp \frac{m}{\sin\theta'} P_n^m \cos(\theta') \begin{matrix}\sin\\ \cos\end{matrix} m\phi'\hat{\phi}\right)\right] \tag{6}$$

$$\bar{N}'^{(2)}(k) = \left[\frac{n(n+1)}{kr'} h_n^{(2)}(kr') P_n^m \cos(\theta') \begin{matrix}\cos\\ \sin\end{matrix} m\phi'\hat{r} + \frac{1}{kr'}\frac{\partial}{\partial(kr')}\left[kr' h_n^{(2)}(kr')\right]\left(\frac{\partial}{\partial\theta'} P_n^m \cos(\theta') \begin{matrix}\cos\\ \sin\end{matrix} m\phi'\hat{\theta} \mp \frac{m}{\sin\theta'} P_n^m \cos(\theta') \begin{matrix}\sin\\ \cos\end{matrix} m\phi'\hat{\phi}\right)\right] \tag{7}$$

and

$$a_n = -\frac{\left[j_n(ka)\right]}{\left[h_n^{(2)}(ka)\right]},\; b_n = -\frac{(d/d\rho))\left[\rho j_n(\rho)\right]}{(d/d\rho)\left[\rho h_n^{(2)}(\rho)\right]},\; \rho = ka \quad \text{and } C_{mn} = (2-\delta_0)\frac{2n+1(n-m)!}{n(n+1)(n+m)!}$$

The radiated fields in vertical and horizontal components are obtained as [3]-[6]

$$E_\theta(r,\theta,\phi) = \frac{e^{-jkr}}{4\pi r}\sum_{n=m}^{\infty} V_m (2-\delta_0)\frac{2n+1}{n(n+1)}\frac{(n-m)!}{(n+m)!} ka^2 (j^{n+1})\cos m\phi (j)\frac{m}{\sin\theta} P_n^m \cos(\theta)\left[\frac{1}{ka}\frac{\partial}{\partial(ka)}\left[ka j_n(ka)\right]\right.$$

$$\left. + a_n \frac{1}{ka}\frac{\partial}{\partial(ka)}\left[ka h_n^{(2)}(ka)\right]\int_{\theta_1-\alpha}^{\theta_1+\alpha} m P_n^m \cos(\theta') d\theta' - \frac{d}{d\theta} P_n^m \cos(\theta)\left[j_n(kr') + b_n h_n^{(2)}(kr')\right]\int_{\theta_1-\alpha}^{\theta_1+\alpha}\frac{d}{d\theta'} P_n^m \cos(\theta')\sin(\theta') d\theta'\right.$$

and

$$E_\phi(r,\theta,\phi) = -\frac{e^{-jkr}}{4\pi r}\sum_{n=m}^{\infty} V_m (2-\delta_0)\frac{2n+1}{n(n+1)}\frac{(n-m)!}{(n+m)!} ka^2 (j^{n+1})\sin m\phi + (j)\frac{d}{d\theta} P_n^m \cos(\theta)\frac{1}{ka}\frac{\partial}{\partial(ka)}\left[ka j_n(ka)\right]$$

$$+ a_n \frac{1}{ka}\frac{\partial}{\partial(ka)}\left[ka h_n^{(2)}(ka)\right]\int_{\theta_1-\alpha}^{\theta_1+\alpha} m P_n^m \cos(\theta') d\theta' - \frac{m}{\sin\theta} P_n^m \cos(\theta)\left[j_n(ka) + b_n h_n^{(2)}(ka)\right]\int_{\theta_1-\alpha}^{\theta_1+\alpha}\frac{d}{d\theta'} P_n^m \cos(\theta')\sin(\theta') d\theta'$$

where the voltage distribution is

$$V_m = \begin{cases} V\dfrac{ka}{(ka)^2 - m^2}\left(\cos(\dfrac{ml}{a}) - \cos kl\right) & ; m \neq 0, m \neq ka \\ V\dfrac{l}{a}\sin kl & ; m = ka \end{cases}$$

4. Radiation Characteristics

4.1 Radiation pattern

The radiation pattern for the effective radius (ka) is obtained from 1 to 20, where a equals the radius of sphere and k is a wave number that is equal to $2\pi/\lambda$ and λ is the wavelengths. They are shown as illustrated in Fig.2. In this paper, we have considered that the slot length is a half-wavelength and the width is infinitesimal. It can be seen from the radiation pattern that for the constant slot dimension, the larger the radius the narrower the beamwidth and the lower the back lobe. At $ka = 1$, the radiated field is very close to the omnidirectional. Moreover, it can be observed that the increasable ka, the radiated field is close to the unidirectional.

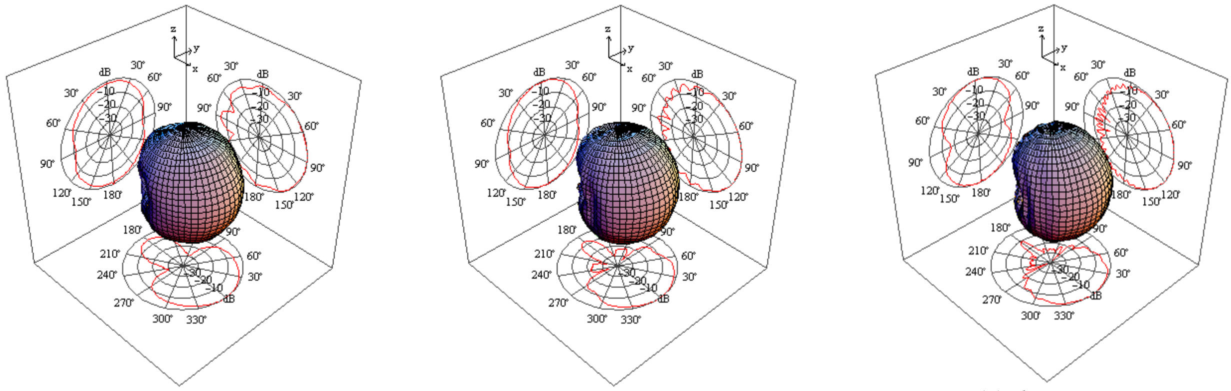

(a) $ka = 5$ (b) $ka = 10$ (c) $ka = 15$

Fig.2 Three dimensional radiation pattern

4.2 Beamwidth

The half-power beamwidth of a slot on conducting sphere is shown in Fig.3. In Fig.3, the half-power beamwidth are illustrated for *xy*, *xz* and *yz* planes. It is obvious that for the effective radius close to zero, the half-power beamwidth is 360 degrees and increase rapidly until to 82 degrees at the effective radius of 3. After that for the larger effective more than 16, the half-power beamwidth become constant at 78 degrees.

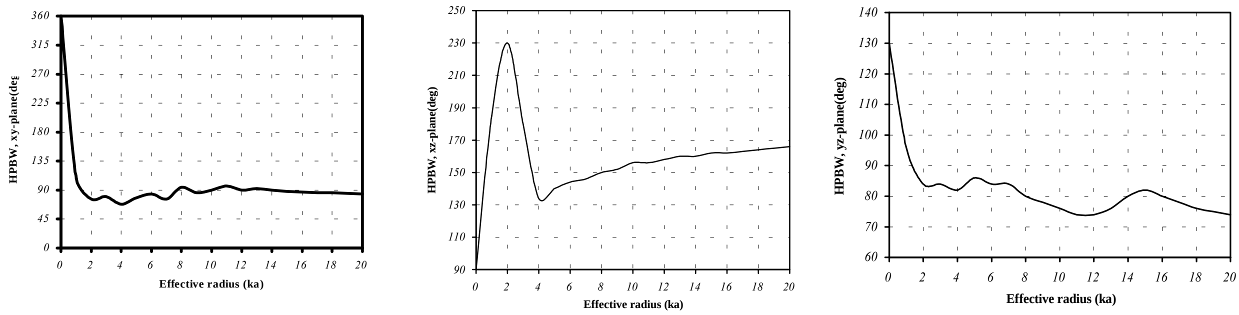

(a) *xy* plane

(b) *xz* plane (c) *yz* plane

Fig.3 Half power beamwidth of a slot on the conducting sphere

4.3 Front-to-back ratio

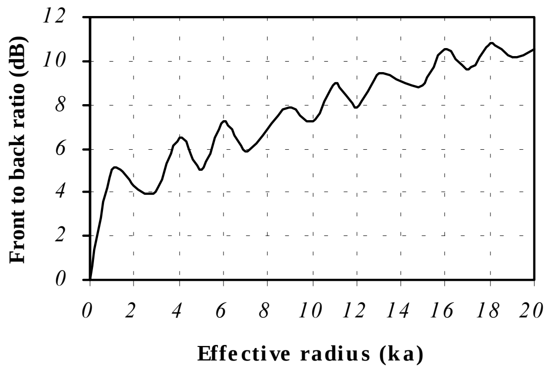

Fig.4 Front-to-back ratio

The front-to-back ratio for various effective radii is shown in Fig.4. It is apparent that the front-to-back ratio is low for the small radius and increase as the large size of the conducting sphere.

4.4 Directivity

The directivity as the function of the effective spherical radius is shown as in the Fig.5. From Fig.5, it is found that the increased variation of effective radius, the directivity is increased slowly as well.

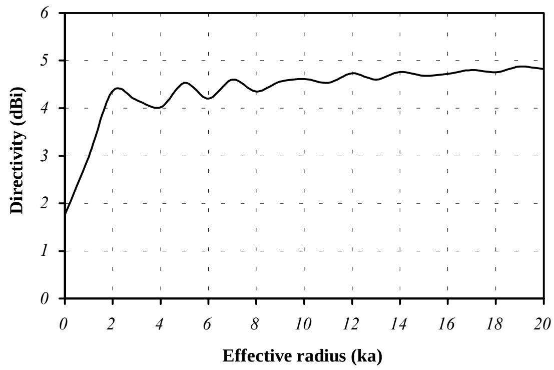

Fig.5 Directivity

5. Experimental Results

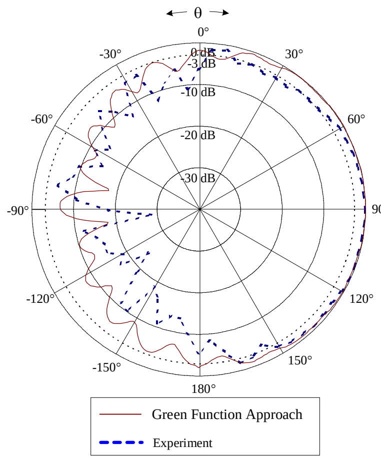

(a) *xz* plane

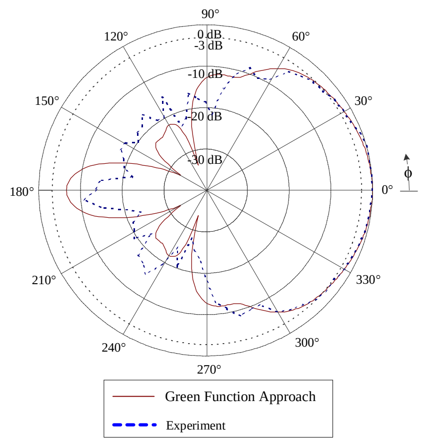

(b) *xy* plane

Fig.6 Comparison between theory and experiment ($ka = 11$)

The experiment is setup to verify the theory. The slot of the length ? cm and width of ? cm is cut on the copper sphere of the radius of ? cm. The radiation pattern in *xz* and *xy* plane are measured to compared with the theoretical results. The compared results are illustrated in Fig.6. It is found that the results are in good agreement in the 3dB region. Hoever, there are some errors in the backward radiation. The reason is that the diffraction phenomena is not taken into account in the calculation.

6. Conclusions

The numerical results of radiation characteristics of the horizontal of a half-wave slot on a conducting sphere such as radiation pattern, half-power beamwidth, front-to-back ratio, directivity are demonstrated. It is apparent that the narrower the half-power beamwidth the higher directivity. The front-to-back ratio reduced by using the larger effective radius of a sphere at a constant slot dimension.

References

[1] Y.Mushiake, and R.E.Webster, "Radiation Characteristics with Power Gain for Slots on a Sphere," *IRE Trans. Antennas Propagat,* vol. AP-5, no.1, pp.47-55, Jan.1957.
[2] C.T.Tai, *Dyadic Green Function in Electromagnetic Theory*, 2nd ed., New York, IEEE Press, 1993.
[3] R.F.Harrington, *Time-Harmonic Electromagnetic Fields*, New York, McGraw-Hill.1961.
[4] C.A.Balanis., *Advanced Engineering Electromagnetic,* John Wiley & Sons, INC.1989.
[5] C.A.Balanis., *Antenna Theory Analysis and Design second edition*, John Wiley & Sons, INC.1997.
[6] M.R.Spiegel, *Theory and Problems of Advanced Mathematics for Engineers & Scientists*, McGraw-Hill, 1988.